Identification of a novel set of scaffolding residues that are instrumental for the inhibitory property of Kunitz (STI) inhibitors

ARTICLE *in* PROTEIN SCIENCE · MARCH 2010

Impact Factor: 2.85 · DOI: 10.1002/pro.338 · Source: PubMed

5 AUTHORS, INCLUDING:

Sudip Majumder
amity university, school of applied sciences
6 PUBLICATIONS **9** CITATIONS
SEE PROFILE

Jhimli Dasgupta
St. Xavier's College, Kolkata
26 PUBLICATIONS **491** CITATIONS
SEE PROFILE

Jiban K Dattagupta
Saha Institute of Nuclear Physics
90 PUBLICATIONS **733** CITATIONS
SEE PROFILE

Udayaditya Sen
Saha Institute of Nuclear Physics
39 PUBLICATIONS **560** CITATIONS
SEE PROFILE

Identification of a novel set of scaffolding residues that are instrumental for the inhibitory property of Kunitz (STI) inhibitors

Susmita Khamrui,[1] Sudip Majumder,[1] Jhimli Dasgupta,[2] Jiban K Dattagupta,[1] and Udayaditya Sen[1,3]*

[1]Crystallography and Molecular Biology Division, Saha Institute of Nuclear Physics, Kolkata 700064, India
[2]Department of Biotechnology, St. Xavier's College, Kolkata 700016, India
[3]Structural Genomics Section, Saha Institute of Nuclear Physics, Kolkata 700064, India

Received 12 October 2009; Revised 16 December 2009; Accepted 17 December 2009
DOI: 10.1002/pro.338
Published online 13 January 2010 proteinscience.org

Abstract: For canonical serine protease inhibitors (SPIs), scaffolding spacer residue Asn or Arg religates cleaved scissile peptide bond to offer efficient inhibition. However, several designed "mini-proteins," containing the inhibitory loop and the spacer(s) with trimmed scaffold behave like substrates, indicating that scaffolding region beyond the spacer is also important in the inhibitory process. To understand the loop-scaffold compatibility, we prepared three chimeric proteins ECI^{L}-WCI^{S}, ETI^{L}-WCI^{S}, and STI^{L}-WCI^{S}, where the inhibitory loop of ECI, ETI, and STI is placed on the scaffold of their homolog WCI. Results show that although ECI^{L}-WCI^{S} and STI^{L}-WCI^{S} behave like good inhibitors, ETI^{L}-WCI^{S} behaves like a substrate. That means a set of loop residues (SRLRSAFI), offering strong trypsin inhibition in ETI, act as a substrate when they seat on the scaffold of WCI. Crystal structure of ETI^{L}-WCI^{S} shows that the inhibitory loop is of noncanonical conformation. We identified three novel scaffolding residues Trp88, Arg74, and Tyr113 in ETI that act as barrier to confine the inhibitory loop to canonical conformation. Absence of this barrier in the scaffold of WCI makes the inhibitory loop flexible in ETI^{L}-WCI^{S} leading to a loss of canonical conformation, explaining its substrate-like behavior. Incorporation of this barrier back in ETI^{L}-WCI^{S} through mutations increases its inhibitory power, supporting our proposition. Our study provides structural evidence for the contribution of remote scaffolding residues in the inhibitory process of canonical SPIs. Additionally, we rationalize why the loop-scaffold swapping is not permitted even among the members of highly homologous inhibitors, which might be important in the light of inhibitor design.

Keywords: chimeric inhibitors; loop and scaffold; crystallography; trypsin inhibition; limited proteolysis; residual enzymatic activity

Introduction

Canonical serine protease inhibitors (SPIs) are widely distributed in nature and based on their global folds these inhibitors can be divided into 20 convergently evolved families.[1] They inhibit their cognate enzymes by binding tightly at the enzyme active site in a substrate-like manner,[2,3] being cleaved extremely slowly compared with a good substrate.[4] The inhibitory loop of the SPIs has a highly conserved canonical structural motif, responsible for

Abbreviations: ECI, *Erythrina variegate* chymotrypsin inhibitor; ECIL-WCIS, chimera having loop of ECI on the scaffold of WCI; ETI, *Erythrina caffra* trypsin inhibitor; ETIL-WCIS, chimera having loop of ETI on the scaffold of WCI; PDB, Protein Data Bank; RMSD, root-mean-square deviation; STI, soybean trypsin inhibitor; STIL-WCIS, chimera having loop of STI on the scaffold of WCI; WCI, winged bean chymotrypsin inhibitor.

**Correspondence to:* Udayaditya Sen, Crystallography and Molecular Biology Division, Saha Institute of Nuclear Physics, 1/AF Bidhannagar, Kolkata 700064, India.
E-mail: udayaditya.sen@saha.ac.in

tight binding with the serine proteases. Comparison of the amino acid sequences of the inhibitory loops indicates a high degree of variability, yet their conformation is quite similar. However, apart from the inhibitory loop, the remaining part of the inhibitor, known as scaffold, has widely different sequence, size, and fold when different families of inhibitors are considered. Now the question comes if the scaffold influences the inhibitory loop to adopt the observed similar conformation, even though the inhibitory loop has quite different set of amino acid sequence for different inhibitors.

Previous investigations on SPIs demonstrated the contribution of a couple of scaffolding residues, encompassed within the inhibitory loop and directly interacting with it, in the inhibitory mechanisms.[5,6] We showed earlier that in Kunitz (STI) family of inhibitors, a scaffolding residue Asn14 forms hydrogen bonds with P2 and P1′ carbonyl O at either side of the scissile peptide bond and holds the cleaved parts together for religation, which is a significant step in the inhibitory mechanism.[5] Through a database analysis, we identified such spacer Asn necessary for religation of the scissile peptide bond in five other families of SPIs, that is, Kazal, SSI, Ecotin, Potato inhibitor-2, and Grasshopper.[5] Furthermore, in chymotrypsin inhibitor-2 (CI2) of the Potato inhibitor-1 family, Arg65 and Arg67 extend in parallel fashion from the protein scaffold to form hydrogen bonds with the inhibitory loop to participate in religation.[6–8] Based on these, several "miniproteins" having trimmed scaffold that host the inhibitory loop were designed, which yielded inhibitors with lesser efficacy, compared with the wild type.[7,9,10] In fact, although CI2 is a potent inhibitor of subtilisin, a synthetic cyclic peptide that mimics the inhibitory loop of CI2 and contains the spacer arginines was turned out to be a substrate of the same enzyme.[7] These results indicate that the role of scaffold in the inhibitory function is not limited only to the spacers, and the contribution of the other parts of the scaffold needs to be investigated.

Chimeric inhibitors having the reactive site loop of one inhibitor on the scaffold of the other could be a good model to understand the extent of loop-scaffold compatibility and hence the role of the scaffold in the inhibitory process. As different families of inhibitors have different folds, it would be logical to restrict this loop-scaffold swapping experiment within one family of inhibitors. We, therefore, took four representative members of Kunitz (STI) family, two of which are chymotrypsin inhibitors, namely, winged bean chymotrypsin inhibitor (WCI)[11] and *Erythrina variegata* chymotrypsin inhibitor (ECI)[12] and other two are trypsin inhibitors, *Erythrina caffra* trypsin inhibitor (ETI)[13,14] and soybean trypsin inhibitor (STI).[15] All of them possess common fold of scaffolds including a conserved Asn, required for religation. Figure 1(a) shows the structure of a representative member, WCI. The inhibitory loop (P4-P4′, shown in magenta) interacts with the enzyme, whereas the scaffolding residue Asn14 acts as a spacer (shown as yellow stick). The scaffold of the inhibitors possesses >80% of the total size but does not make any direct contact with enzyme. Our aim was to replace the inhibitory loop (P4-P4′) of WCI with that of ECI, ETI, and STI through site-directed mutagenesis to see how these modified inhibitory loops are accommodated by the scaffold of WCI in terms of canonical conformation and inhibitory property, keeping in mind that the inhibitory loops have high tolerance to the sequence variability.

Initially, we replaced the P1 Leu of WCI by Arg and the mutant L65R was found to be a potent inhibitor of trypsin.[16] Using L65R as a starting point, here, we prepared the chimeric proteins ETI^{L}-WCI^{S} (having reactive site loop of trypsin inhibitor ETI on the scaffold of WCI), STI^{L}-WCI^{S} (having reactive site loop of trypsin inhibitor STI on the scaffold of WCI), and their intermediate mutants following the scheme, shown in Figure 1(b,c). Another chimera ECI^{L}-WCI^{S} (having reactive site loop of ECI on the scaffold of WCI) was also prepared. Crystallographic studies were performed on the chimeric proteins ECI^{L}-WCI^{S} and STI^{L}-WCI^{S}, and the inhibitory property of all the mutants [Fig. 1(c)] has been judged. Our structural observations, when coupled with the results of limited proteolysis and the residual enzymatic activity, identified a set of novel scaffolding residues, extended beyond the conventional spacer residue(s), which are instrumental in maintaining the conformation of the binding loop, thereby influencing the inhibitory property. We further showed how the inhibitors belonging to one phylogenic group use a unique set of scaffolding residues in combination with a particular set of inhibitory loop residues and rationalized why the loop-scaffold swapping is not permitted even among the members of highly homologous inhibitors.

Results

Inhibitory property and cleavage pattern of the chimeric proteins and the intermediate mutants

ETI^{L}-WCI^{S} and the intermediate mutants. Four mutations at the inhibitory loop (P3, P2, P1, and P2′) of WCI are required to prepare the chimeric protein ETI^{L}-WCI^{S} [Fig. 1(b,c)]. Our previous study showed that a single mutation at P1 (L65R) converted WCI to a potent trypsin inhibitor.[16] We have performed additional three mutations in a stepwise manner on L65R to obtain the chimeric protein ETI^{L}-WCI^{S} [Fig. 1(c)]. To our surprise, the mutant, F64L/L65R, where P2 and P1 of WCI are replaced with the residues of ETI, shows lesser inhibition to

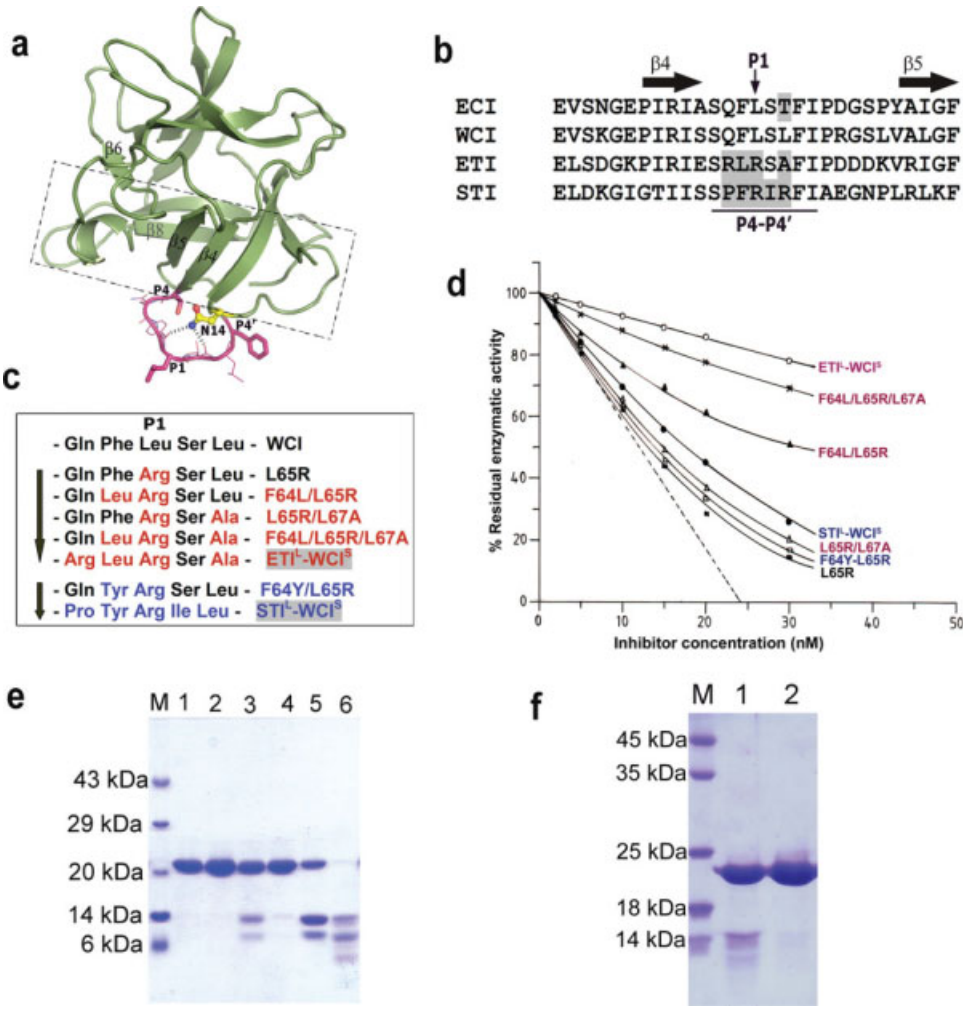

Figure 1. (a) The reactive site loop (P4-P4′; magenta) and the scaffold (green) of winged bean chymotrypsin inhibitor (WCI). The extended scaffold is denoted as dotted box, and the beta strands of the extended scaffold are marked. The spacer residue Asn14 (yellow ball-and-stick) and the reactive site loop residues are shown. The hydrogen bonds made by the ND2 atom of Asn14 with P1 and P1′ carbonyl O are shown as dotted lines. (b) Sequence alignment of ECI, ETI, and STI with WCI around the reactive site loop (P4-P4′) region. The reactive site loop residues, which are different from that of WCI, are shaded. The neighboring beta strands and the P1 residue are indicated. (c) The mutagenesis scheme for preparation of the chimeric proteins and the intermediate mutants. The mutants prepared in a stepwise manner toward ETI^L-WCI^S are represented in red, whereas those for STI^L-WCI^S are in blue. The final chimeras in both cases are marked in gray. (d) Inhibition of estarolytic activity of trypsin by the mutants. Trypsin (25 n*M*) was incubated at 25°C for 15 min with varying amounts (2–30 n*M*) of inhibitors, and the residual enzymatic activity was assayed at A_{410}, taking 2.5 m*M* BAPNA as substrate. (e) Limited proteolysis of the WCI mutants by trypsin is analyzed in a 15% SDS-PAGE. L65R is mixed with trypsin in 50:1 (Lane No. 1) and 100:1 (Lane No. 2) molar ratio. The other mutant inhibitors (F64L/L65R, Lane No. 3; L65R/L67A, Lane No. 4; F64L/L65R/L67A, Lane No. 5; ETI^L-WCI^S, Lane No. 6) are mixed with trypsin in 100:1 molar ratio. The reaction was performed at 25°C for 6 h. The molecular weight of the proteins used as markers (Lane No. M) is indicated. (f) A total of 15% SDS-PAGE showing the limited proteolysis of STI^L-WCI^S (Lane No. 1) and F64Y/L65R (Lane No. 2) by trypsin. The inhibitors are mixed with trypsin in a 100:1 molar ratio and incubated for 6 h at 25°C. Molecular weight of the proteins used as marker (Lane No. M) is indicated. [Color figure can be viewed in the online issue, which is available at www.interscience.wiley.com.]

trypsin compared with L65R [Fig. 1(d)]. However, another double mutant L65R/L67A, where P1 and P2′ of WCI are replaced with the residues of ETI, shows better inhibition compared with the previous double mutant F64L/L65R [Fig. 1(d)]. The cleavage pattern of these two double mutants, seen in the limited proteolysis study with trypsin, corroborates their residual enzymatic activity data [Fig. 1(d,e)]. The chimera is of 186 residues (that includes three residues from cloning artifact) and cleavage at the scissile bond (after Arg65) by trypsin produces two bands ~14 and ~7 kDa in SDS page, as seen in Figure 1(e,f). F64L/L65R, the P2/P1 mutant, shows considerable cleavage, whereas L65R/L67A, the P1/P2′ mutant, shows negligible cleavage when incubated with trypsin for 6 h at 25°C [Fig. 1(e)]. No cleavage was observed for L65R under similar condition [Fig. 1(e)]. Interestingly, the triple mutant

F64L/L65R/L67A and the quadruple mutant ETI^{L}-WCI^{S} show gradual increment of cleavage and lesser residual enzymatic activity profile [Fig. 1(d,e)]. In fact, ETI^{L}-WCI^{S} behaves almost like a substrate of trypsin [Fig. 1(d,e)].

STI^{L}-WCI^{S} and the intermediate mutants. Five mutations, at all five subsites (P3 to P2′) of the inhibitory loop, are required to convert WCI to STI^{L}-WCI^{S} [Fig. 1(b)], and we performed four mutations on the P1 mutant L65R to prepare the chimera STI^{L}-WCI^{S} [Fig. 1(c)]. Residual enzyme activity and limited proteolysis studies have been performed on the P2/P1 double mutant F64Y/L65R and the chimera STI^{L}-WCI^{S}. In contrast to the substrate-like behaviors of ETI^{L}-WCI^{S}, STI^{L}-WCI^{S} shows considerable inhibitory activity, as evident from the residual enzymatic activity and limited proteolysis data [Fig. 1(d,f)]. F64Y/L65R also shows residual enzyme activity and cleavage pattern, which is comparable to L65R [Fig. 1(d,f)].

ECI^{L}-WCI^{S}. L67T, a single mutation at P2′ converted WCI to the chimeric protein ECI^{L}-WCI^{S}. The structure of the chimeric protein ECI^{L}-WCI^{S} was not determined here, but the inhibitory activity of ECI^{L}-WCI^{S} and its resistance toward proteolysis against chymotrypsin are measured. Both of these values are comparable to that of WCI (data not shown), implying that the ECI^{L}-WCI^{S} also acts as a good inhibitor of chymotrypsin.

Structure of the chimeric proteins

ETI^{L}-WCI^{S}. Overall, the structure of the scaffold of the chimera ETI^{L}-WCI^{S} matches with that of WCI both in the 12 beta strands and the surface loop regions, except at the inhibitory loop. The inhibitory loop of ETI^{L}-WCI^{S} adopts a conformation, which is neither like that of WCI (PDB code: 1EYL) nor like that of ETI (PDB code: 1TIE) or L65R (PDB code: 1XG6) [Fig. 2(a)]. The conformational difference in ETI^{L}-WCI^{S} inhibitory loop is observed mainly in the P1–P4 region [Table I, Fig. 2(a)]. The P3 residue of ETI, WCI, and L65R is seen to be solvent exposed, whereas in ETI^{L}-WCI^{S}, P1–P4 region of the inhibitory loop is folded back toward the scaffold in such a way that the C_{α} of P3 moves about 2.6 Å toward the scaffold and the side chain of P3 Arg comes close to Trp90 (that corresponds to Trp88 of ETI) forming π-electron interactions [Fig. 2(b)]. The movement of P3 Arg is such that its guanidium group roughly approximates the position of Arg74 of ETI [Fig. 2(b)]. These features have been grossly observed in both the molecules of the asymmetric unit [Fig. 2(b)], although there are some differences in conformation. Furthermore, Glu111 of the scaffold has been observed in two different side chain conformations in the two molecules of the asymmetric unit to make hydrogen bond with the guanidium group of P3 Arg, which is disposed in slightly different mode.

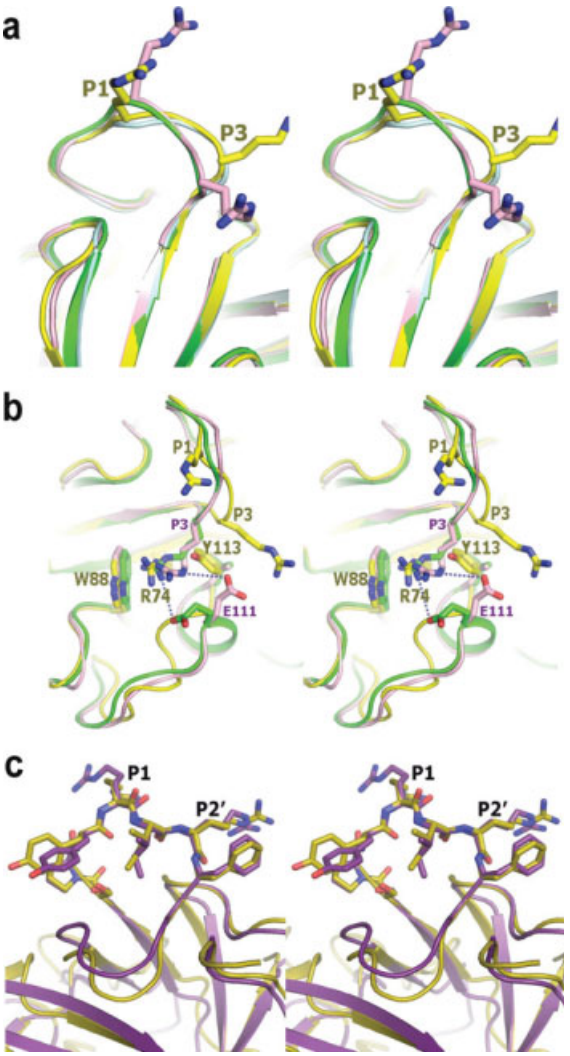

Figure 2. (a) Comparison of the reactive site loop conformation of ETI^{L}-WCI^{S} with ETI and L65R. The two molecules in the asymmetric unit of ETI^{L}-WCI^{S} are shown in green and pink, ETI in yellow, and L65R in sky blue. P1 and P3 residues are shown in stick. (b) Conformation of the P3 Arg, reactive site loop and the extended scaffold of ETI^{L}-WCI^{S} and ETI. The hydrogen-bonding interactions are represented by dotted lines. Color code is same as Figure 3(a). (c) Comparison of the reactive site loop conformation of STI^{L}-WCI^{S} (gold) with STI (violet). [Color figure can be viewed in the online issue, which is available at www.interscience.wiley.com.]

STI^{L}-WCI^{S}. As expected, the scaffold of the chimeric protein STI^{L}-WCI^{S} matches well with that of WCI, but the inhibitory loop of this chimera, in both the molecules in the asymmetric unit, adopts a conformation, very similar to the inhibitory loop of STI (Table I). On an average, the inhibitory loop (P4-P4′) can be superposed with a root-mean-square deviation (RMSD) value of 0.24 Å. Interestingly, the

Table I. *Dihedral Angles (φ/ψ) Around the Reactive Site Loop in ETI, STI, and Related Chimeras*

	P4	P3	P2	P1	P1′	P2′	P3′	P4′
ETI and ETI chimera								
ETI	−88/172	−66/−31	−113/151	−67/135	−169/152	−75/−46	−106/164	−103/134
ETIL-WCIS	−88/−11	58/29	−123/175	−95/58	−129/150	−78/−20	−124/−175	−131/108
	−82/−8	69/10	−113/157	−80/87	−154/151	−73/−25	−130/−179	−131/117
STI and STI chimera								
STI	−113/150	−71/−29	−62/159	−84/22	−61/148	−91/−23	−128/127	−69/112
STIL-WCIS	−114/130	−59/−35	−63/153	−81/59	−114/148	−78/−39	−117/154	−96/113
	−93/145	−79/0	−91/162	−88/71	−137/166	−102/−38	−110/142	−80/120

similarity is observed not only at the main-chain level but also all the side chains of the inhibitory loop adopt a conformation similar to those of STI. However, the inhibitory loop of STI^{L}-WCI^{S} superposes on that of STI showing a hinge motion of the former [Fig. 2(c)]. When compared with the reactive site loop of WCI, it has been observed that maximum structural change of STI^{L}-WCI^{S} occurs at P3 Pro, which, on an average, has been displaced by ~2.5 Å from WCI to acquire the canonical inhibitory loop conformation of STI. The average hydrogen bonding distance between ND2 atom of the scaffolding residue Asn14 and the carbonyl oxygens of P2 and P1′ is weaker (~3.3 Å) compared with WCI (~2.9 Å). These two hydrogen bonds were implicated in the religation of the peptide bond after it is being cleaved by the enzyme.[5]

The role of Arg74 and Tyr113 of ETI and their verification. Our structural results, when combined with the scrutiny of ETI structure, identified a set of residues from ETI scaffold, Arg74, Trp88, and Tyr113 (Fig. 3), which stacks together to restrain the flexibility of the inhibitory loop. Absence of this barrier in ETI^{L}-WCI^{S} causes a movement of P3 Arg toward Trp90 (that corresponds to Trp88 of ETI)

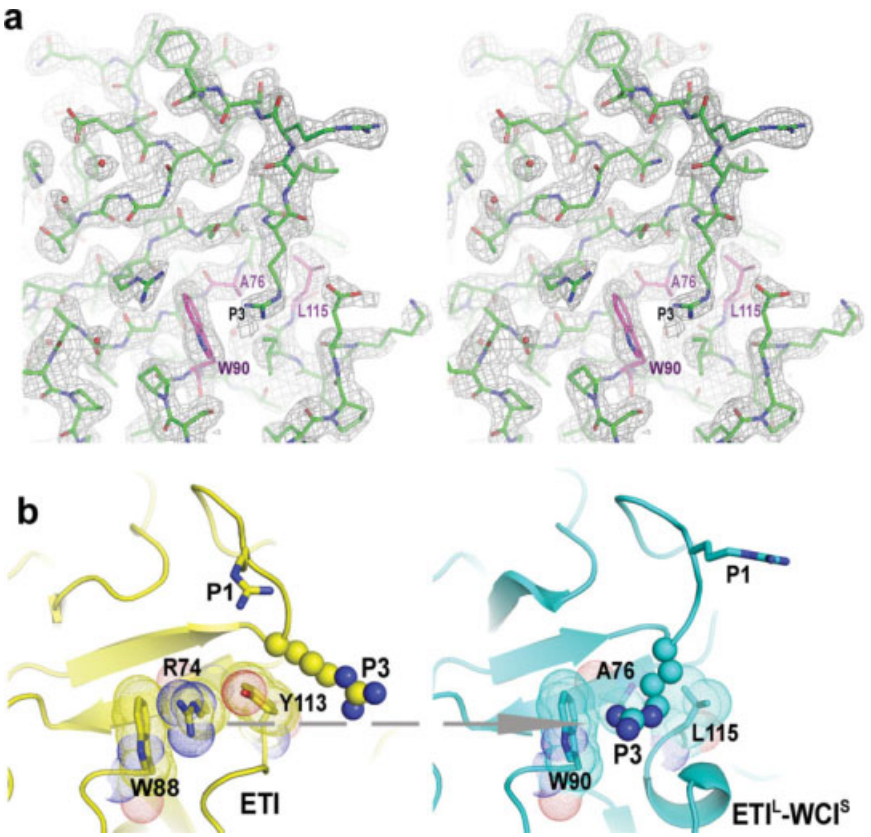

Figure 3. (a) Stereoscopic representation of a $2F_o - F_c$ electron density map, contoured at 1.2 ó, overlaid on the inhibitory loop and its neighboring scaffold in ETI^{L}-WCI^{S}. Residues corresponding to the barrier residues of ETI are shown in magenta and labeled. P3 Arg is also labeled. (b) Orientation of P3 Arg in the presence of scaffolding barrier in ETI (yellow), and the movement of P3 Arg in the absence of such a scaffolding barrier in ETI^{L}-WCI^{S} (cyan). Arrow indicates the loss of barrier from ETI to ETI^{L}-WCI^{S}. [Color figure can be viewed in the online issue, which is available at www.interscience.wiley.com.]

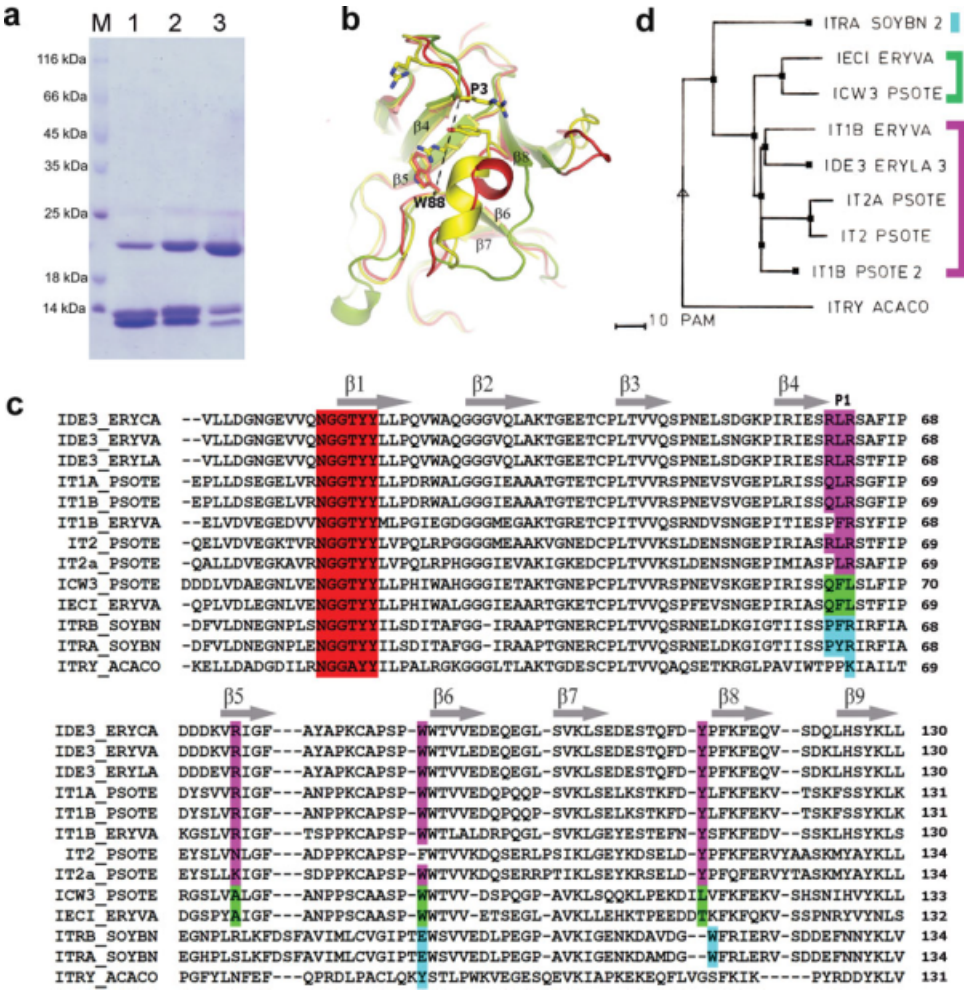

Figure 4. (a) A 15% SDS-PAGE showing the limited proteolysis of ETI^{L}-WCI^{S} (Lane No. 1), A76R on ETI^{L}-WCI^{S} (Lane No. 2), and L115Y/A76R on ETI^{L}-WCI^{S} (Lane No. 3) by trypsin in 100:1 molar ratio (inhibitor/enzyme) for 6 h at 25°C. The molecular weight of the proteins used as markers (Lane No. M) is indicated in the figure. (b) Structural difference between ETI (Yellow), WCI (Red), and STI (Green) at the loops ($^{\beta5}L_{\beta6}$ and $^{\beta7}L_{\beta8}$) near the inhibitory loop. The distance between P3 Arg and Trp88 for ETI is indicated by dotted line. (c) Sequence alignment of the trypsin and chymotrypsin inhibitors from Kunitz (STI) family performed with Blast. The set of loop residues that are in combination with the set of scaffolding residues are marked in similar color like magenta (ETI type), green (WCI type), and cyan (STI type). (d) Dendogram of the predicted tree of the trypsin and chymotrypsin inhibitors belonging to Kunitz (STI) family. The program MULTALIN was used to draw the dendogram. [Color figure can be viewed in the online issue, which is available at www.interscience.wiley.com.]

[Fig. 3(a,b)]. To verify this observation, we made two more mutations A76R and A76R/L115Y at equivalent positions on ETI^{L}-WCI^{S} scaffold. Limited proteolysis study on these mutants shows that the single mutant A76R undergoes lesser cleavage compared with ETI^{L}-WCI^{S}, and the double mutant A76R/L115Y shows substantially lesser cleavage compared with ETI^{L}-WCI^{S}, implying considerable improvement in the inhibitory property [Fig. 4(a)].

Discussion

During inhibition, the inhibitory loop (P4-P4′) of the SPIs makes most of the contacts with its cognate enzyme, whereas the scaffold of the inhibitor barely makes contact with the enzyme and if there is any that is mostly nonspecific. Previous investigations on canonical SPIs demonstrated the role of a few spacer residues, which are engaged either in shaping up of the inhibitory loop or in the religation process of the cleaved scissile peptide bond.[5,6] However, several lines of evidences[7,9,10] suggested that beside a couple of proximal spacer residue(s), the role of the other part of the scaffold needs to be investigated. Here, we performed structural and biochemical studies on the chimeric proteins, having loops of ETI, STI, and ECI on the scaffold of WCI (ETI^{L}-WCI^{S}, STI^{L}-WCI^{S}, and ECI^{L}-WCI^{S}) along with some of the intermediate mutants. To level the religation contribution of conserved spacer Asn14, it was kept unchanged in all chimeras. The results, therefore, helped us to figure out the role of the structural elements of the extended part of the scaffold

participating in inhibitory process. At the beginning, we mutated P1 Leu of WCI to Arg (L65R) and that point mutant became a potent inhibitor of trypsin.[16] The inhibitory efficiency of L65R is in n*M* range (with an association constant, K_a value of 4.8×10^{10} M^{-1})[16] although it is still slightly less potent compared with ETI[17] and STI[14] whose K_a values are 3.8×10^{11} M^{-1} and 1×10^{11} M^{-1}, respectively. The P2/P1 double mutant F64Y/L65R, which is an intermediate of STI^L-WCI^S, also inhibits trypsin to a similar extent like L65R [Fig. 1(d)]. At this point, expecting that the other required mutations at the inhibitory loop [Fig. 1(b,c)] will convert WCI to trypsin inhibitors as potent as ETI or STI, we prepared the chimeric proteins ETI^L-WCI^S and STI^L-WCI^S. In contrast, we observed that although STI^L-WCI^S shows substantial inhibition to trypsin, ETI^L-WCI^S behaves almost like a substrate of trypsin [Fig. 1(d–f)]. To understand the reason behind the substrate-like behavior of ETI^L-WCI^S, we systematically investigated the inhibitory property of its intermediate mutants. Limited proteolysis experiment shows that cleavage of the triple mutant F64L/L65R/L67A (intermediate of ETI^L-WCI^S) is significant, and noticeable biochemical cleavage begins at the corresponding P2/P1 double mutant, F64L/L65R. However, the maximum cleavage is observed in case of ETI^L-WCI^S [Fig. 1(e)]. Results of the residual enzymatic activity also follow the same trend as of limited proteolysis [Fig. 1(d)]. Therefore, it is evident that, on the way of preparing the chimera ETI^L-WCI^S, mutation at P3 causes maximum damage to the loop conformation and inhibitory property. The structure of the scaffold of ETI^L-WCI^S, which is basically the scaffold of WCI, matches to a large extent to the scaffold of ETI as they are homologous proteins. However, the reactive site loop of ETI^L-WCI^S, having amino acid sequences identical to that of ETI, adopts a conformation significantly different from that of ETI (Fig. 3). Our structural results when combined with the scrutiny of ETI structure identified a set of residues from ETI scaffold, Arg74, Trp88, and Tyr113 (Fig. 3). These three residues stack together and act as a barrier for the inhibitory loop to confine the movement of the carboxy terminal region (P4–P1) of the scissile peptide bond to keep the inhibitory loop in its canonical conformation. The scaffolding residues that are forming the barrier in ETI (Arg74, Trp88, and Tyr113) are Ala76, Trp90, and Leu115, respectively, in WCI and hence also in the chimera ETI^L-WCI^S. As a result, the P4–P1 region of ETI^L-WCI^S faces a different spatial and chemical environment compared with ETI. Leu115 and Ala76 in ETI^L-WCI^S, which are the close neighbors of P3 Arg, are smaller than their ETI counterpart. Therefore, the barrier that confines the P4–P1 portion of the loop in ETI is lost in case of ETI^L-WCI^S, and its P3 Arg gets more room to move toward Trp90 [Fig. 2(a,b)]. The movement of P3 Arg in ETI^L-WCI^S is such that its guanidium group roughly approximates the position of Arg74 of ETI [Figs. 2(b) and 3]. In its new conformation, P3 Arg also interacts weakly with Glu111 [Fig. 2(b)]. This conformation has consistently been observed in both the molecules of the asymmetric unit. In spite of this conformational change in the P3 part of the inhibitory loop, in the uncleaved state Asn14 is still in a position to hydrogen bond with the carbonyl oxygen of P2 and P1′. However, in the cleaved inhibitors, if we consider the movement of P3 Arg toward Trp90 [Fig. 2(a,b)], it may be difficult for Asn14 to maintain the hydrogen bonds with the carbonyl oxygen of P2 and P1′ to religate the scissile peptide bond.

Cleavage of the scissile peptide bond and subsequent increase in the inhibitory loop mobility have been observed in case CI2.[18] Moreover, it is known that loss of intramolecular functional coupling between the surface loop and the protein core decreases inhibitory potency.[19] Therefore, it seems to us that the inhibitory loop conformation of ETI^L-WCI^S is recognized by trypsin and cleavage occurs at scissile bond; however, because of the incompatibility of the inhibitory loop and the scaffold of this chimera, the inhibitory loop acquires added mobility after the cleavage and Asn14 becomes unable to religate the scissile peptide bond, making ETI^L-WCI^S a substrate of trypsin.

Arg74, Trp88, and Tyr113 of ETI work together to shape up and more importantly to restrain the flexibility of the inhibitory loop [Fig. 2(b)]. To verify our proposition, we made two more mutants A76R and A76R/L115Y on ETI^L-WCI^S scaffold expecting that these mutations would fill up the vacant space between P3 Arg and Trp90 restricting the inhibitory loop from unwanted movement. Limited proteolysis study on these mutant shows that the single mutant undergoes lesser cleavage compared with ETI^L-WCI^S, whereas the double mutant shows substantially lesser cleavage compared with the chimera, implying considerable improvement in the inhibitory property [Fig. 4(a)]. Therefore, the double mutant A76R/L115Y is providing much lesser space for the movement of P3 Arg creating a chemical environment more reminiscent to ETI, which supports our proposition. Slight cleavage seen in the double mutant A76R/L115Y is probably due to not-so-precise disposition of Tyr115 side chain, compared with ETI, which is caused because of the slight difference in C_α positions between Tyr115 of the double mutant and the corresponding Tyr113 of ETI.

In STI, the conformation of the inhibitory loop is not constrained by the extended loop scaffold interactions as observed in ETI. The residue at P3 of STI is Pro, which has an inherent rigidity causing a restriction of the loop mobility. In addition, the side chain of P3 Pro makes hydrophobic interactions

with Trp117, a scaffolding residue specific for STI. On the other side of the scissile peptide bond, P2′ Arg makes ionic interactions with Glu12 of the scaffold. In STI^L-WCI^S the inhibitory loop (P4-P4′) possesses ϕ/ψ values quite similar to that of STI (Table I), and they can be superposed with an RMSD value of 0.2 Å. In STI^L-WCI^S side chain of P3 Pro makes hydrophobic contacts with Leu115, and residue P2′ Arg makes ionic interactions with Glu13 of the scaffold. Despite these similarities in loop structure and loop-scaffold interaction, STI^L-WCI^S inhibits trypsin to slightly lesser extent ($K_a = 1.51 \times 10^{10}$ M^{-1}) than STI ($K_a = 1 \times 10^{11}$ M^{-1}) indicating that there are still some fine differences in loop-scaffold compatibility, which is responsible for lesser inhibition.

STI, ETI, ECI, and WCI consist of 12 beta strands connected by loops, and the inhibitory loop is situated at the loop $^{\beta4}L_{\beta5}$ that joins strands β4 and β5. The loops, $^{\beta5}L_{\beta6}$ and $^{\beta7}L_{\beta8}$, are the nearest neighbors of the inhibitory loop, and we see that these loops are different for the three inhibitors [Fig. 4(b)]. In case of ETI and WCI, $^{\beta7}L_{\beta8}$ is close to the inhibitory loop but it takes totally different conformation in STI and stays away from the inhibitory loop [Fig. 4(b)]. In ETI, Trp88 from $^{\beta5}L_{\beta6}$, Arg74 from β5, and Tyr113 from $^{\beta7}L_{\beta8}$ act as barrier for the inhibitory loop and restrain the conformation of P3 Arg and the inhibitory loop as a whole. Amongst them Trp88 is farthest from the inhibitory loop, being ~14 Å away from P3 Arg [Fig. 4(b)]. We have done a sequence comparison using only the Kunitz (STI) family of inhibitors (as different families of inhibitors have different amino acid sequences and folds), which indicates that only a few combinations of residues at P3-P2-P1 positions are possible, and these are R-L-R, Q-L-R, and P-Y/F-R/K for trypsin inhibitors and Q-F-L for chymotrypsin inhibitors [Fig. 4(c)]. Interestingly, inhibitors that have a combination of R-L-R or Q-L-R (ETI type) in the loop need a support from the scaffold in the form of a barrier, and for these inhibitors the barrier is present in the form of $W(^{\beta5}L_{\beta6})...R/N/K(\beta5)...Y(^{\beta7}L_{\beta8})$ [Fig. 4(c)]. On the other hand, for the combination of residues Q-F-L at the inhibitory loop (WCI type), corresponding scaffolding residues are W..A...L/V [Fig. 4(c)]. Interestingly for the combination of loop residues P-Y/F-R/K (STI type) the barrier is no longer required, partly because of the conformational restriction imposed by P3 Proline and its packing with conserved Trp117. Therefore, within the homologous family of Kunitz (STI), although conserved motif NGGTYY [Fig. 4(c)] provides the spacer Asn14 to participate in religation, scaffolding residues further away from Asn14 influence the reactive site loop conformation by acting as barrier.

Kunitz (STI) family of inhibitors can also be grouped based on their phylogenic relationships [Fig. 4(d)]. Structural and biochemical results when coupled with phylogenic analysis indicate that the inhibitors belonging to one group use a unique set of loop residues for inhibition and they do so in combination with a highly specified set of scaffold residues, implying that the loop and scaffold are not independent unit, rather they work in tandem to make an efficient inhibitor. Presumably, an inhibitory loop did not evolve independently, but the scaffold was also evolved in accordance with the loop making inhibitors of precise specificity and high efficacy. In our study, chimera ETI^L-WCI^S behaves like a substrate of trypsin rather than an inhibitor. However, the double mutant A76R/L115Y on ETI^L-WCI^S gives the scaffold a closer resemblance to that of ETI rather than WCI, and this mutant occurs to be a more potent inhibitor of trypsin in comparison to the chimera ETI^L-WCI^S. Therefore, we can say that by introducing these mutations, we have been able to increase the "inhibitory potency" of ETI^L-WCI^S to a greater extent, and this information can be viewed as a case of "conformational epistasis"[20] where introduction of some lost contacts helps to resurrect a functionality at a particular site by readjusting the conformational backbone of the protein at another site.

In conclusion, our study identified a novel set of remote scaffolding residues that directly influence the inhibitory loop conformation for Kunitz (STI) inhibitors. Furthermore, we showed that even amongst the members of highly homologous inhibitors the loop-scaffold swapping is not permitted. However, swapping has a varying degree of effect depending on amino acid compositions of the inhibitory loop. When loop has an in-built stability loop-scaffold swapping is still permitted although in this case also, inhibitory potency is compromised. These results might be useful to understand the general mechanism of inhibition and in the inhibitor design.

Materials and Methods

Site-directed mutagenesis, expression, and purification

The mutation primers were designed (purchased from Neuprocell) to replace the loop/scaffolding residues as indicated in Figure 1. Mutagenesis experiments were performed following the protocols described earlier.[16] The clones were confirmed through sequencing and subcloned in $pET28a^+$ for overexpression. The mutant proteins were expressed in *E. coli* BL21 (DE3) cells as fusion protein, having a 6xHis-tag at the N-terminus followed by a thrombin cleavage site, in the presence of kanamycin. In each case, the His_6-tagged protein was purified from the cell lysate by Ni-NTA affinity column. The His_6-tag was cleaved by thrombin and the protein was further purified by gel filtration, using Sephacryl S-

100 (GE Healthcare) column (78 cm × 1.4 cm), preequilibrated with a buffer, containing 50 m*M* Tris (pH 8.0), 100 m*M* NaCl, and 0.02% NaN_3 at 4°C. The homogeneity of the purified proteins was checked in 12% SDS-PAGE.

Crystallization and data collection

The chimeric protein ETI^L-WCI^S was concentrated to 15–20 mg/mL in 50 m*M* acetate buffer (pH 4.6) containing 100 m*M* NaCl. Crystal growth was accomplished using the hanging drop vapor diffusion method against 700 μL of reservoir and incubated at 20°C using 5% PEG 6K in 0.1*M* MES (pH 6.0) as precipitant against 20% PEG 6K. STI^L-WCI^S was concentrated to ~30 mg/mL in buffer containing 100 m*M* NaCl in 50 m*M* Tris at pH 8.0 and was crystallized in 5% PEG 6K in 0.1*M* citrate (pH 7.0) as precipitant against 20% PEG 6K as reservoir. X-ray diffraction data for ETI^L-WCI^S and STI^L-WCI^S were collected up to the resolutions of 2.85 and 2.3 Å, respectively, using MAR345 research image-plate detector with copper K_α radiation, generated by a Bruker-Nonius FR591 rotating-anode generator, equipped with Osmic MaxFlux confocal optics, running at 50 kV and 90 mA. For ETI^L-WCI^S, the crystals were briefly soaked in a solution containing 5% glycerol and 5% PEG 6K in 0.1*M* MES, pH 6.0, and flash frozen in a stream of nitrogen (Oxford cryo-system) at 100 K. For STI^L-WCI^S, the crystals were briefly soaked in a solution containing 10% glycerol and 5% PEG 6K in 0.1*M* citrate, pH 7.0. Data were processed and scaled using the program suite AUTOMAR (http://www.marresearch.com/automar/run/htm). The data collection and processing statistics are given in Table II.

Structure determination and refinement

Structures of the chimeric proteins were solved by Molecular Replacement using MOLREP of CCP4 suite.[22] Both for ETI^L-WCI^S and STI^L-WCI^S, crystal structure of free state L65R (PDB code: 1XG6) was used as a search model, yielding two molecules in the asymmetric unit for both the cases with space group symmetry C2 and I4 (Table II), respectively. The structures were refined by alternating cycles of model rebuilding and refinement using "O" (version 7.2)[23] and CNS.[24] The progress of refinement was monitored by checking the R_{free} value (5% of the reflections were excluded out of refinement as R_{free} for cross-validation). Cycles of positional refinement combined with simulated annealing refinement produced good R_{free} for both the structures (Table II). The final structures have been validated by using omit map in CNS, which produced excellent electron density maps for in each cases.

Assay of trypsin inhibitory activity

The trypsin inhibitory activity of ETI^L-WCI^S, STI^L-WCI^S, and their intermediates was estimated using the synthetic substrate *N*-α-*p*-benzoyl-*p*-nitroanilide (BAPNA). The trypsin inhibitory activity can be estimated by measuring the decreasing rate of linear release of the *p*-nitroanilide at 410 nm[25] with increasing amount of the inhibitors. The reagents, bovine β-trypsin, BAPNA, Tris, and $CaCl_2$ were bought from Sigma, and DMSO was bought from Merck. All the reactions were performed in the buffer of 0.04*M* Tris (pH 8.1) containing 0.01*M* $CaCl_2$. The stock solutions of trypsin and the inhibitors were 250 n*M* in the same buffer. The stock solution of BAPNA was prepared by dissolving it into DMSO to a final concentration of 25 m*M*. Temperature for these inhibitory reactions was set at 25°C, and all the spectrophotometric measurements were done in Unicam UV–vis absorption spectrophotometer.

To determine the residual enzymatic activity, 25 n*M* of trypsin was preincubated with increasing amount of the loop mutants ranging from 2 to 30 n*M* for 15 min in a final reaction volume of 500 μL. After incubation, the residual enzymatic activity was measured by monitoring the rate of the reaction at A_{410} using 2.5 m*M* BAPNA for 300 s. The ratio of the product release in presence of the inhibitors to the product release in absence of the inhibitor is determined as the residual enzymatic activity and

Table II. *Data Collection and Refinement Statistics*

	ETI^L-WCI^S	STI^L-WCI^S
Data collection statistics		
Space group	C2	I4
Cell dimensions (Å, °)	a = 71.80 Å; b = 40 Å; c = 121.55 Å; β = 101.33°	$a = b$ = 141.38 Å; c = 46.72 Å
Molecule(s)/ASU	2	2
Mathews coefficient, V_m ($Å^3$/Da)	2.046	2.779
Completeness (%)	92.1 (92.8)[a]	96.1 (92.9)
R_{merge} (%)	9.6 (17.3)	3.7 (18.8)
Resolution (Å)	20–2.85	20–2.3
Mosaicity	0.3	0.3
Average redundancies	2.35 (2.36)	2.88 (2.69)
Average I/σ	4.1 (2.7)	7.8 (3.1)
Crystal to detector distance (mm)	280	200
Oscillation (°)	0.5	0.5
R_{cryst} (%)[b]	22.5	23.4
R_{free} (%)[b]	28.5	28.9
RMSD[c] bond (Å)	0.008	0.006
RMSD bond (°)	1.9	1.6
Ramachandran plot (%)[d]		
Most favored (%)	78.9	87.8
Allowed (%)	21.1	12.2
Disallowed (%)	0	0

[a] Values in parenthesis correspond to the outermost resolution shell.
[b] $R_{cryst} = \Sigma_{hkl}||F_o| - |F_c||/\Sigma_{hkl}|F_o|$, 5% of the reflections were excluded for the R_{free} calculation.
[c] RMSD, root-mean-square-deviation.
[d] Analyzed by PROCHECK.[21]

plotted against the inhibitor concentration. All the experiments were done in triplicate to minimize the experimental error.

Limited proteolysis

Limited proteolysis experiments were carried out to investigate the possible cleavage of the loop mutants by trypsin. The experiment was set up at 25°C using an enzyme/inhibitor ratio of 1:100 (w/w). A total of 0.01 mg/mL of trypsin was incubated with 1 mg/mL of inhibitor for 6 h in 0.04*M* Tris (pH 8.1) containing 0.01*M* $CaCl_2$, the same buffer used in determining the residual enzymatic activity study. After 6 h of incubation, the reaction was terminated by the addition of an equal volume of 2× sample buffer consisting of 0.25*M* Tris-HCl (pH 6.8), 20% glycerol, 0.005% bromophenol blue, 4% SDS, and 10% 2-mercaptoethanol followed by immediate boiling to 100°C. The cleavage pattern was analyzed by running them into a 15% SDS-PAGE.

Accession numbers

The coordinates and structure factors have been deposited at the PDB with following PDB IDs: STI^L-WCI^S—3I2A; ETI^L-WCI^S—3I2X.

References

1. Krowarsch D, Cierpicki T, Jelen F, Otlewski J (2003) Canonical protein inhibitors of serine proteases. Cell Mol Life Sci 60:2427–2444.
2. Laskowski M, Jr, Kato I (1980) Protein inhibitors of proteinases. Annu Rev Biochem 49:593–626.
3. Bode W, Huber R (1992) Natural protein proteinase inhibitors and their interaction with proteinases. Eur J Biochem 204:433–451.
4. Radisky ES, Koshland DE, Jr (2002) A clogged gutter mechanism for protease inhibitors. Proc Natl Acad Sci USA 99:10316–10321.
5. Dasgupta J, Khamrui S, Dattagupta JK, Sen U (2006) Spacer Asn determines the fate of Kunitz (STI) inhibitors, as revealed by structural and biochemical studies on WCI mutants. Biochemistry 45:6783–6792.
6. Radisky ES, Lu CJ, Kwan G, Koshland DE, Jr (2005) Role of the intramolecular hydrogen bond network in the inhibitory power of chymotrypsin inhibitor 2. Biochemistry 44:6823–6830.
7. Radisky ES, King DS, Kwan G, Koshland DE, Jr (2003) The role of the protein core in the inhibitory power of the classic serine protease inhibitor, chymotrypsin inhibitor 2. Biochemistry 42:6484–6492.
8. Radisky ES, Kwan G, Karen LuC J, Koshland DE, Jr (2004) Binding, proteolytic, and crystallographic analyses of mutations at the protease-inhibitor interface of the subtilisin BPN′/chymotrypsin inhibitor 2 complex. Biochemistry 43:13648–13656.
9. Mucsi Z, Gáspári Z, Orosz G, Perczel A (2003) Structure-oriented rational design of chymotrypsin inhibitor models. Protein Eng 16:673–681.
10. Gururaja TL, Narasimhamurthy S, Payan DG, Anderson DC (2000) A novel artificial loop scaffold for the noncovalent constraint of peptides. Chem Biol 7: 515–527.
11. Dattagupta JK, Podder A, Chakrabarti C, Sen U, Dutta SK, Singh M (1996) Structure of a Kunitz-type chymotrypsin from winged bean seeds at 2.95 A resolution. Acta Crystallogr D 52(Part 3):521–528.
12. Iwanaga S, Nagata R, Miyamoto A, Kouzuma Y, Yamasaki N, Kimura M (1999) Conformation of the primary binding loop folded through an intramolecular interaction contributes to the strong chymotrypsin inhibitory activity of the chymotrypsin inhibitor from *Erythrina variegata* seeds. J Biochem 126:162–167.
13. Onesti S, Brick P, Blow DM (1991) Crystal structure of a Kunitz-type trypsin inhibitor from *Erythrina caffra* seeds. J Mol Biol 217:153–176.
14. Laskowski M, Jr, Fankenstadt WR (1972) Study of protein-protein and or protein-ligand interaction by potentiometric methods. Methods Enzymol 26:193–237.
15. Song HK, Suh SW (1998) Kunitz-type soybean trypsin inhibitor revisited: refined structure of its complex with porcine trypsin reveals an insight into the interaction between a homologous inhibitor from *Erythrina caffra* and tissue-type plasminogen activator. J Mol Biol 275:347–363.
16. Khamrui S, Dasgupta J, Dattagupta JK, Sen U (2005) Single mutation at P1 of a chymotrypsin inhibitor changes it to a trypsin inhibitor: X-ray structural (2.15 Å) and biochemical basis. Biochim Biophys Acta 1752: 65–72.
17. Onesti S, Matthews DJ, Aducci P, Amiconi G, Bolognesi M., Menegatti E, Ascenzi P (1992) Binding of the Kunitz-type trypsin inhibitor DE-3 from *Erythrina caffra* seeds to serine proteinases: a comparative study. J Mol Recognit 5:105–114.
18. Shaw GL, Davis B, Keeler J, Fersht AR. (1995) Backbone dynamics of chymotrypsin inhibitor 2: effect of breaking the active site bond and its implications for the mechanism of inhibition of serine proteases. Biochemistry 34:2225–2233.
19. Szenthe B, Patthy A, Gáspári Z, Kékesi AK, Gráf L, Pál G. (2007) When the surface tells what lies beneath: combinatorial phage-display mutagenesis reveals complex networks of surface-core interactions in the pacifastin protease inhibitor family. J Mol Biol 370:63–79.
20. Ortlund EA, Bridgham JT, Redinbo MR, Thornton JW (2007) Crystal structure of an ancient protein: evolution by conformational epistasis. Science 317: 1544–1548.
21. Laskowski RA, MacArthur MW, Moss DS, Thornton JM (1993) PROCHECK: a program to check the stereochemical quality of protein structures. J Appl Crystallogr 26:283–291.
22. Collaborative Computational Project, Number 4 (1994) The CCP4 suite: programs for protein crystallography. Acta Crystallogr Sect D 50:760–763.
23. Jones TA, Zou JY, Cowan SW, Kjeldgaard M (1991) Improved methods for building protein models in electron density maps and the location of errors in these models. Acta Crystallogr Sect A 47:110–119.
24. Brünger AT, Adams PD, Clore GM, DeLano WL, Gros P, Grosse-Kunstleve RW, Jiang J-S, Kuszewski J, Nilges M, Pannu NS, Read RJ, Rice LM, Simonson T, Warren GL (1998) Crystallography and NMR system: a new software suite for macromolecular structure determination. Acta Crystallogr D 54:905–921.
25. Erlanger BF, Kokowsky N, Cohen W (1961) The preparation and properties of two new chromogenic substrates of trypsin. Arch Biochem Biophys 95: 271–278.